Synthetic gauge potential and effective magnetic field in a Raman medium undergoing molecular modulation

Luqi Yuan,[1] Da-wei Wang,[2] and Shanhui Fan[1]

[1]*Department of Electrical Engineering and Ginzton Laboratory, Stanford University, Stanford, California 94305, USA*

[2]*Department of Physics and Astronomy and Institute for Quantum Science and Engineering, Texas A&M University, College Station, Texas 77843, USA*

(Received 13 November 2016; published 1 March 2017)

We theoretically demonstrate nontrivial topological effects for a probe field in a Raman medium undergoing molecular modulation processes. The medium is driven by two noncollinear pump beams. We show that the angle between the pumps is related to an effective gauge potential and an effective magnetic field for the probe field in the synthetic space consisting of a synthetic frequency dimension and a spatial dimension. As a result of such an effective magnetic field, the probe field can exhibit a topologically protected one-way edge state in the synthetic space, as well as Landau levels which manifest as suppression of both diffraction and sideband generation. Our work identifies a previously unexplored route towards creating topological photonics effects and highlights an important connection between topological photonics and nonlinear optics.

DOI: 10.1103/PhysRevA.95.033801

I. INTRODUCTION

The process of molecular modulation [Fig. 1(a)] has attracted significant interest in the last two decades [1–9]. In this process, molecules are driven by two pump fields, which generate coherence between a few low-lying vibrational and/or rotational levels through a Raman transition. A probe field couples with the molecular coherence, which results in the generation of Raman sidebands. This process is highly efficient and has found applications in attosecond pulse generation [10], coherent broadband light generation [11,12], and optical orbital angular momentum transfer [13,14].

Most previous experiments on molecular modulation assume a collinear propagation between the pump and the probe [Fig. 1(b)]. In this paper, we consider a pump configuration as shown in Fig. 1(c), where two pump beams are assumed to be noncollinear, with both their directions near the z axis, subtending an angle $\alpha \ll 1$ rad. We show that when a probe beam propagating along the z axis is introduced into this medium, such a molecular coherence results in a synthetic gauge field that couples to the probe field. As a result, the probe field exhibits a nontrivial topological photonic effect including a topologically protected one-way edge state along the frequency axis, as well as Landau levels which manifest as suppression of both diffraction and sideband generation.

Explorations of synthetic gauge potential [15–22] and topological effects [23–33] for light have generated significant recent interest since these effects open a new dimension in the control of the flow of light. Most previous works on synthetic gauge field and topological photonics rely upon complex material geometries. In contrast, here we show that topological photonic effects naturally arise in a standard nonlinear optics geometry. Our work points to a fruitful direction at the interface between nonlinear optics and topological photonics. Related to this work, a noncollinear beam configuration was previously used to generate a synthetic gauge field in real space for neutral atoms [34–36]. Also, the use of a classical electromagnetic field to generate a gauge potential was explored in the context of phonon-photon coupling [37]. Our work differs in that we focus on a synthetic space rather than a real space. The predicted effects also represent a mechanism for controlling Raman sidebands in a system exhibiting molecular coherence.

II. THEORETICAL ANALYSIS

We start our analysis by considering a molecular Raman-active medium. The molecules have a ground state [labeled a in Fig. 1(a)], a low-lying excited state (labeled b), and intermediate states (labeled i) at higher energies. The medium is driven by two pump laser pulses, centered at frequencies ω_A and ω_B, respectively. The pumps are nonresonant with respect to any molecular transitions but are two-photon near resonant with the a-b transition with a small detuning $\Delta\omega \equiv (\omega_b - \omega_a) - (\omega_A - \omega_B)$. The pumps create a coherence ρ_{ab} between levels a and b. Here, we focus on the interaction of a probe field with such coherence. Therefore, we adopt the analytic model that was used in [2,4,38], where both the pumps and the probe are treated as continuous wave at a single frequency, and we discuss the experimental setup, including the choice of the appropriate pulse parameters, towards the end of the paper.

The propagation equation for a laser beam at frequency ω is [4,38]

$$\frac{\partial}{\partial z}E_\omega - i\frac{c}{2\omega}\frac{\partial^2}{\partial x^2}E_\omega = ic\mu_0\hbar\omega P_\omega. \tag{1}$$

Here, we assume the beam propagates near the z axis and use the paraxial wave approximation. μ_0 is the vacuum permeability, and E_ω and P_ω are the slowly varying envelopes for the spectral components of the electric field and the polarization, respectively, at the frequency ω.

For the pumps $E_{A(B)}$, we use the solution of P_ω in Refs. [2,4,38] and write Eq. (1) as

$$\frac{\partial}{\partial z}E_{A(B)} - i\frac{c}{2\omega_{A(B)}}\frac{\partial^2}{\partial x^2}E_{A(B)} = ic\mu_0\hbar\omega_{A(B)}N\left[a_{\omega_{A(B)}}\rho_{aa} + d_{\omega_{A(B)}}\rho_{bb}\right]E_{A(B)}, \tag{2}$$

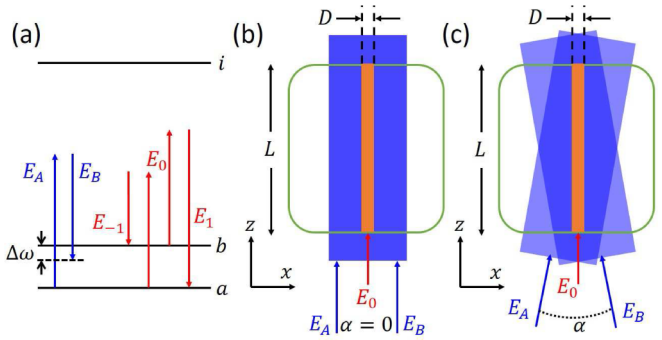

FIG. 1. (a) Energy levels of a molecule used in the molecular modulation process. Levels a and b are ground states, and i are the excited states. Pump fields E_A and E_B are far from resonance between the ground states and the excited states but are near resonance with the two-photon transition a-b. Sidebands E_n are generated via the interaction of molecular coherence ρ_{ab} as generated from the pump with the probe field E_0. (b) and (c) Pump fields and the probe field are injected into the Raman-active medium (inside a cell in the green square with a length L) along the z direction. Two pump fields (blue regions) propagate collinearly at an angle $\alpha = 0$ in (b) and noncollinearly at $\alpha = 0.5^\circ$ in (c). The probe field (red arrow) has a focal area at $z = 0$ which is much smaller than the beam waist of the pump fields. The simulation region has a width D and is shown in orange.

where N is the number density of the molecule. In Eq. (2),

$$a_\omega = \frac{1}{2\hbar^2}\sum_i\left[\frac{|\mu_{ai}|^2}{(\omega_i-\omega_a)-\omega}+\frac{|\mu_{ai}|^2}{(\omega_i-\omega_a)+\omega}\right], \quad (3)$$

$$d_\omega = \frac{1}{2\hbar^2}\sum_i\left[\frac{|\mu_{bi}|^2}{(\omega_i-\omega_b)-\omega}+\frac{|\mu_{bi}|^2}{(\omega_i-\omega_b)+\omega}\right], \quad (4)$$

where $\mu_{a(b)i}$ is the dipole moment between levels a and b and intermediate state i. In Eq. (2) we keep only the first-order perturbation to the pumps because we are interested in the sideband generation from the probe. Because the pumps are nonresonant with respect to any molecular transition, we have $a_{\omega_{A(B)}} \cong d_{\omega_{A(B)}} \cong a_0$. By using $\rho_{aa}+\rho_{bb}=1$, Eq. (2) becomes

$$i\frac{\partial}{\partial z}E_{A(B)} = -\kappa_{A(B)}\frac{\partial^2}{\partial x^2}E_{A(B)} - \beta_{A(B)}E_{A(B)}, \quad (5)$$

where $\kappa_{A(B)} = c/2\omega_{A(B)}$ and

$$\beta_{A(B)} = c\mu_0\hbar\omega_{A(B)}Na_0. \quad (6)$$

Therefore, the pump fields in general can be described as a Gaussian or Hermite-Gaussian beam with the wave vector $k_{A(B)}+\beta_{A(B)}$.

The pumps create coherence ρ_{ab} between levels a and b, which oscillates at the frequency $\omega_m = \omega_A - \omega_B$ [see Fig. 1(a)] with an amplitude of [2,4,38]

$$\rho_{ab} = \frac{1}{2}\frac{b_{\omega_A}E_AE_B^*}{\sqrt{|b_{\omega_A}E_AE_B^*|^2+\Delta\omega^2}}, \quad (7)$$

where

$$b_\omega = \frac{1}{2\hbar^2}\sum_i\left[\frac{\mu_{ai}\mu_{bi}^*}{(\omega_i-\omega_a)-\omega}+\frac{\mu_{ai}\mu_{bi}^*}{(\omega_i-\omega_b)+\omega}\right]. \quad (8)$$

To study the propagation of the probe, based on the experimental scenarios described above, we assume that the coherence does not decay as the weak probe field propagates through the medium. The probe has the carrier frequency ω_0. When the probe interacts with the coherence in the medium, sidebands at frequencies $\omega_n = \omega_0 + n\omega_m$ are generated, where n is an integer. From Eq. (1), the propagation equation for the electric field in the nth sideband E_n is [2,4,38]

$$\frac{\partial}{\partial z}E_n - i\frac{c}{2\omega_n}\frac{\partial^2}{\partial x^2}E_n = ic\mu_0\hbar\omega_n N\{[a_{\omega_n}\rho_{aa}+d_{\omega_n}\rho_{bb}]E_n + b^*_{\omega_n}\rho_{ab}E_{n-1}+b_{\omega_{n+1}}\rho^*_{ab}E_{n+1}\}, \quad (9)$$

where a_ω and d_ω are defined in Eqs. (3) and (4) and b_ω is defined in Eq. (8). Since all the sidebands are sufficiently far from any resonance, again, we have

$$a_{\omega_n} \cong d_{\omega_n} \cong a_0, \quad b_{\omega_n} \cong b_0. \quad (10)$$

Therefore, Eq. (9) simplifies to

$$i\frac{\partial}{\partial z}E_n = \beta_nE_n - \kappa_n\frac{\partial^2}{\partial x^2}E_n - g_n(2\rho_{ab}E_{n-1}+2\rho^*_{ab}E_{n+1}), \quad (11)$$

where $\kappa_n = c/2\omega_n$, $\beta_n = c\mu_0\hbar\omega_nNa_0$, and $g_n = c\mu_0\hbar\omega_nNb_0/2$.

From Eq. (7), with the pump configuration as described in Fig. 1(c), we have

$$\rho_{ab}(x,z) = \frac{1}{2}\frac{|b_{\omega_A}E_A(x)E_B^*(x)|}{\sqrt{|b_{\omega_A}E_A(x)E_B^*(x)|^2+\Delta\omega^2}}e^{i\theta(x)}e^{-i(\beta_A-\beta_B)z}, \quad (12)$$

where

$$\theta(x) = qx, \quad (13)$$

with $q \approx \alpha(k_A+k_B)/2$. On the other hand, from Eq. (6), one can show that $\beta_n - \beta_{n-1} = \beta_m = \beta_A - \beta_B$. Therefore, we perform the transformation $E_n = \tilde{E}_n\exp(i\beta_nz)$ and $\rho_{ab} = \tilde{\rho}_{ab}\exp(i\beta_mz)$ to obtain

$$i\frac{\partial}{\partial z}\tilde{E}_n = -\kappa\frac{\partial^2}{\partial x^2}\tilde{E}_n - g(x)(e^{iqx}\tilde{E}_{n-1}+e^{-iqx}\tilde{E}_{n+1}). \quad (14)$$

In arriving at Eq. (14), we note that in the limit of $\omega_0 \gg \omega_m$, $\kappa_n \cong \kappa$ and $2g_n|\rho_{ab}| \cong g$ [39].

III. EFFECTIVE GAUGE POTENTIAL FOR THE PROBE IN THE SYNTHETIC SPACE

To understand the physics in Eq. (14), we apply a gauge transformation $\tilde{E}_n = \varepsilon_ne^{inqx}$, define a continuous function $\varepsilon(\omega,x)$ such that $\varepsilon(\omega_n,x) = \varepsilon_n$, and approximate the term in the parentheses by a continuous derivative. Equation (14) becomes

$$i\frac{\partial}{\partial z}\varepsilon(\omega,x) \approx \kappa\left(-i\frac{\partial}{\partial x}+\frac{\omega-\omega_0}{\omega_m}q\right)^2\varepsilon(\omega,x) + g\omega_m^2\left(-i\frac{\partial}{\partial\omega}\right)^2\varepsilon(\omega,x) - 2g\varepsilon(\omega,x). \quad (15)$$

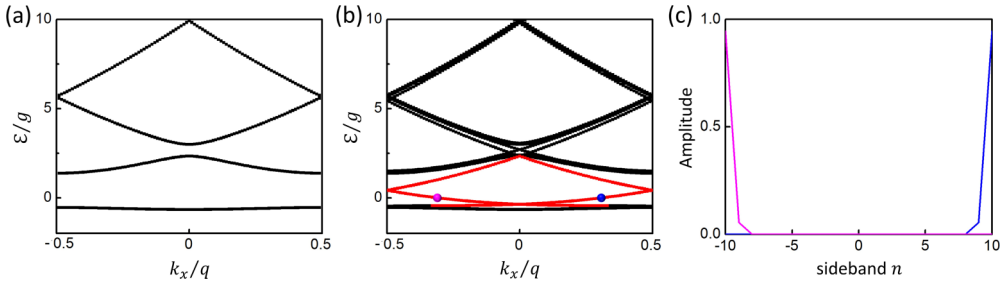

FIG. 2. (a) The projected band structure within the first Brillouin zone $k_x \in [-q/2,q/2]$ in an infinite system described by Eq. (14). We choose $\kappa = g(\pi/2q)^2$. (b) The projected band structure in a 2D strip that is infinite along the x axis but with a finite number of sidebands (sideband number $n = -10,\ldots,10$) along the frequency dimension. In the lowest band gap, there exists two one-way edge modes (shown in red). (c) Field amplitudes of the two edge modes shown by purple and blue dots in (b).

Equation (15) has the form of a Schrödinger equation in $2+1$ dimensions, except with the usual time axis being replaced by the z axis and with the remaining two dimensions describing a *synthetic space* with one spatial dimension along the x direction and one synthetic frequency dimension [40,41]. In this synthetic space, Eq. (15) describes an effective gauge potential $A_\omega = (\omega - \omega_0)q/\omega_m$ along the x axis, which gives a uniform effective magnetic field orthogonal to the two-dimensional (2D) space:

$$B = \frac{\partial A}{\partial \omega} = \frac{q}{\omega_m} = \alpha\frac{(k_A + k_B)}{2\omega_m}. \tag{16}$$

To examine the topological effect created by such an effective magnetic field, we calculate the band structure of an infinite 2D system described by Eq. (14) with a uniform $g(x) = g$ along the x direction. Equation (14) has a spatial periodicity of $2\pi/q$ along the x axis as well as a symmetry with respect to the translational operation n to $n+1$ along the frequency axis. Therefore, it can be described in terms of a band structure $\mathcal{E}(k_x,k_\omega)$, which relates the wave-vector shift for the probe $\mathcal{E}$ along the z direction to the quantum numbers k_x and k_ω, corresponding to the translational symmetries as described above. We take $\kappa = g(\pi/2q)^2$ and plot the projected band structure within the first Brillouin zone $k_x \in [-q/2,q/2]$ in Fig. 2(a). Due to the effective magnetic field, for each k_x the bands are almost completely flat along the k_ω axis. Therefore, the projected bands appear as lines in the $\mathcal{E}$-k_x plane. The bulk bands here correspond to the Landau level of a particle under a constant magnetic field. In the continuum limit [such as described by Eq. (15)] the bands would be completely flat along both the k_x and k_ω axes. Here the nonzero slope along the k_x axis arises from the discrete translational symmetry.

The bands in Fig. 2(a) are topologically nontrivial as characterized by nonzero Chern numbers [42]. Therefore, in a strip geometry there should be topologically protected one-way edge states within the gap. As a demonstration, we consider a strip that is infinite along the x axis but with finite numbers of n ($n = -10,\ldots,10$) along the frequency axis. We plot its band structure $\mathcal{E}(k_x)$ in Fig. 2(b). In the lowest band gap, there exists two one-way edge modes. The field amplitudes corresponding to the two edge modes at $\mathcal{E} = 0$ [labeled by purple and blue dots in Fig. 2(b)] are shown in Fig. 2(c). The band-structure analysis here indeed shows the nontrivial topology when the pumps are noncollinear.

IV. NUMERICAL DEMONSTRATIONS OF ONE-WAY EDGE STATE AS WELL AS LANDAU LEVELS

While topological effects have been observed in a wide variety of photonic systems, the process of molecular modulation provides a unique aspect of probing topological effects. To illustrate these effects, in what follows we will solve Eq. (14) numerically for several different pump and probe configurations. The parameters used in our simulations are based on recent experiments on either the gas medium [3,4,6] or the Raman-active crystal [11,12]. The molecular density is chosen to be $N \sim 10^{18}$–10^{19} cm^{-3}. The frequencies of the pump and probe lasers are of the order of 1 μm. Given these conditions, we have $g \sim 10^2$–10^3 m^{-1}, $\kappa \sim 10^{-7}$ m. At $z = 0$, the probe field has a spatial profile of

$$f(x) = e^{-(x/\Delta x)^2}, \tag{17}$$

with a focal width $\Delta x = 38.8\,\mu$m. We will study the propagation of this probe field along the z axis.

In Fig. 3 we present the simulation results for the system with a noncollinear pump geometry with $\alpha = 0.5^\circ$, which gives $q = 5\times10^4$ m^{-1}. We choose $\kappa \sim 10^{-7}$ m and $g = 10^2$ m^{-1}. These parameters are the same as those used for generating the band structure in Fig. 2(b). The beam waists of the pump fields are chosen to be $w_0 = 1$ mm, which corresponds to the Rayleigh length $z_R \sim 3$ m. The length of the medium is $L = 5$ cm. We perform the simulation in a $D \times L$ region as represented by the orange rectangle in Fig. 1(c), with $D = 0.433$ mm, because the probe field does not diffract out of this region in the entire simulation. Since $D < w_0$ and $L \ll z_R$, we assume that the amplitudes of the pump fields are uniform in the simulation region, so the coherence is also uniform along the x direction in Eq. (14). In order to create an edge along the frequency axis, we add two-level atoms to the system that provides additional frequency dispersion. We choose two-level atoms to have a resonant frequency $\omega_{99} - 0.025\omega_m$, a density of 2.5×10^{15} cm^{-3}, and a dephasing rate $1/T_2 = 10^{10}/2\pi$ s^{-1}. Here, ω_n is the frequency of the nth sideband frequency satisfying $\omega_n = (n+0.8)\omega_m$. The wave vector β as a function of frequency near the resonant frequency of the two-level atoms is shown in Fig. 3(a). Such two-level atoms strongly influence the wave vectors at the 99th sideband without influencing the wave vector of 100th sideband. With such a choice we expect that the 100th sideband cannot down-convert, which creates a boundary along the

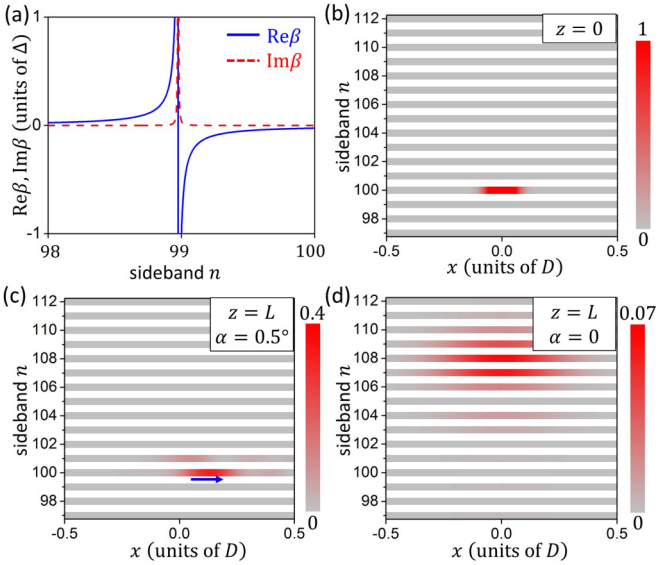

FIG. 3. (a) The wave vector mismatching for the probe along the z direction $\beta(\omega_n)$ with an additional two-level atom added into the medium at a resonant frequency $\omega_{99} - 0.025\omega_m$. $\Delta = 10^3$ m^{-1}. (b) The normalized intensity as a function of position and sidebands for the input probe field. The input field has a frequency of $100.8\omega_m$. (c) and (d) The output field intensity at $z = L$, corresponding to the noncollinear pump geometry in Fig. 1(c) and the collinear pump geometry in Fig. 1(b). The blue arrow in (c) indicates the propagation direction of the edge state.

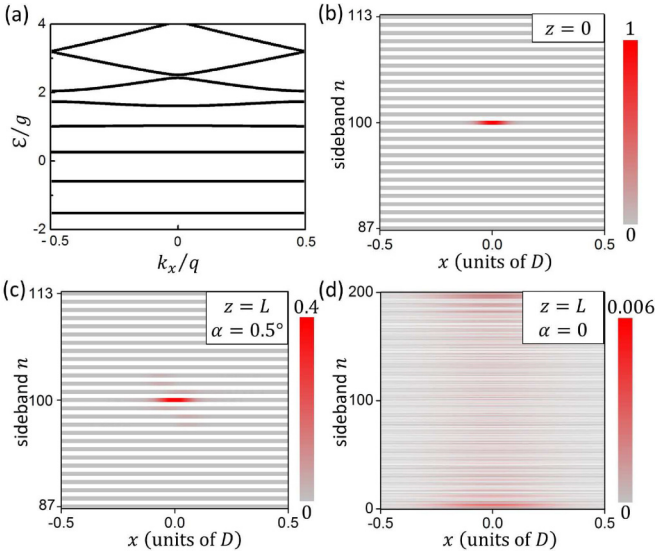

FIG. 4. (a) The projected band structure showing the formation of Landau levels. $\kappa = 0.1g(\pi/2q)^2$. (b) The normalized intensity as a function of position and sidebands for the input probe field. The input field has a frequency of $100.8\omega_m$. (c) and (d) The output field intensity at $z = L$, corresponding to the noncollinear pump geometry in Fig. 1(c) and the collinear pump geometry in Fig. 1(b).

frequency axis. In the simulation, we input at $z = 0$ a beam at ω_{100}, and we consider 16 sidebands from ω_{97} to ω_{112} [Fig. 3(b)]. After propagation, the beam shifted towards the $+x$ direction and showed very little frequency conversion, consistent with the existence of a one-way edge state localized at the lowest frequency boundary [Fig. 3(c)]. As a comparison, we study the evolution of the probe with a collinear pump geometry, i.e., $\alpha = 0$, while keeping all the other parameters the same as in Fig. 3(c) [see Fig. 1(b)]. In the case where the input probe frequency is $100.8\omega_m$ [Fig. 3(b)], we observe significant diffraction and frequency conversion [Fig. 3(d)]. In the collinear pump geometry there is no effective magnetic field, and hence, there is no one-way edge state.

For electrons in two dimensions, an important consequence of a perpendicular magnetic field is the existence of Landau level, a bulk band with its energy completely independent of the in-plane wave vectors. For photons, the Landau level has been observed in [19], which relies upon a sophisticated dielectric geometry. In contrast, here, we show that our system can directly generate the Landau level for photons (Fig. 4). As an illustration, here, we choose a larger $g = 10^3$ m^{-1} and keep all other system parameters as in Fig. 3, except without the additional two-level atoms. In general, the underlying band structure of the system, in the absence of the effective magnetic field, is a tight-binding band along the frequency axis. The use of a larger g ensures that such a tight-binding band can be approximated by a parabolic band over a large range of $\mathcal{E}$, which facilitates the creation of the Landau level in the presence of the effective magnetic field. Figure 4(a) shows the projected bulk band-structure calculation for the system shown in Fig. 1(c), which supports an effective magnetic field. We indeed observe that the lowest five bands are almost completely flat in the k_x and k_ω planes, signifying the creation of the Landau level. As a demonstration of the effect of the Landau level, we input the same probe beam as in Fig. 3, but with a frequency centered at $100.8\omega_m$, as shown in Fig. 4(b). We see that the probe field does not diffract in the spatial dimension and also shows no frequency conversion [Fig. 4(c)]. This is direct evidence of Landau levels; the flattened bands prevent diffraction as well as frequency conversion. Our system here provides a mechanism to guide light with light. Unlike conventional waveguides, in which light is guided in a well-defined core region, here, guiding occurs for every spatial and spectral position inside the "bulk." We compare our results with the evolution of the probe with a collinear pump geometry, i.e., $\alpha = 0$ [Fig. 1(b)]. In this case, we choose the same input probe beam as shown in Fig. 4(b). Significant diffraction and frequency conversion occurs, as seen in Fig. 4(d).

V. DISCUSSION AND CONCLUSION

In the simulations above, we treat the probe field in Eq. (14) as a monochromatic field. Our results are also valid if the pumps and the probe are pulses, as long as the temporal duration of the pulses are long such that the slowly varying envelope approximation is valid. Using a long pump pulse, the coherence can be prepared via the "adiabatic following" scheme [43]. We give an example of typical time scales of pulses in a possible experiment. For the pump one can use an ~500-fs pulse, which has a spectral width of $\delta\omega_{\mathrm{FWHM}}/\omega_{\mathrm{pump}} \sim 10^{-3}$. For such a pump one can assume that q is a constant in Eq. (13). To study the interaction of a probe pulse with the coherence, one can send in the probe pulse at a time delay. For the probe, one can use an ~500-fs pulse at a

time delay of ∼1 ps with respect to the pump. At such a time delay the coherence has not decayed [44]. Alternatively, one can also use long pump pulses of ∼1 ns and send the probe into the medium while the pumps are on. In this case, one can choose the frequencies of the pump and the probe to be sufficiently different and study the propagation of the probe.

In summary, we studied the process of the coherent Raman sideband generation using molecular modulation with a noncollinear pump geometry. We showed that such a geometry can provide a synthetic gauge potential and achieve nontrivial topological effects. Our work identifies a previously unexplored route towards creating topological photonics effects and highlights an important connection between topological photonics and nonlinear optics.

ACKNOWLEDGMENTS

The authors acknowledge stimulating discussions with Prof. S. Harris. This work is supported by U.S. Air Force Office of Scientific Research Grant No. FA9550-12-1-0488.

[1] R. W. Boyd, *Nonlinear Optics*, 3rd ed. (Academic, Burlington, MA, 2008).
[2] S. E. Harris and A. V. Sokolov, Phys. Rev. Lett. **81**, 2894 (1998).
[3] A. V. Sokolov, D. R. Walker, D. D. Yavuz, G. Y. Yin, and S. E. Harris, Phys. Rev. Lett. **85**, 562 (2000).
[4] A. V. Sokolov and S. E. Harris, J. Opt. B **5**, R1 (2003).
[5] D. D. Yavuz, D. R. Walker, and M. Y. Shverdin, Phys. Rev. A **67**, 041803(R) (2003).
[6] S. W. Huang, W.-J. Chen, and A. H. Kung, Phys. Rev. A **74**, 063825 (2006).
[7] D. D. Yavuz, Phys. Rev. A **75**, 041802(R) (2007).
[8] T. Suzuki, M. Hirai, and M. Katsuragawa, Phys. Rev. Lett. **101**, 243602 (2008).
[9] Y. Y. Wang, C. Wu, F. Couny, M. G. Raymer, and F. Benabid, Phys. Rev. Lett. **105**, 123603 (2010).
[10] S. Baker, I. A. Walmsley, J. W. G. Tisch, and J. P. Marangos, Nat. Photonics **5**, 664 (2011).
[11] M. Zhi and A. V. Sokolov, Opt. Lett. **32**, 2251 (2007).
[12] K. Wang, M. Zhi, X. Hua, J. Strohaber, and A. V. Sokolov, Appl. Opt. **53**, 2866 (2014).
[13] J. Strohaber, M. Zhi, A. V. Sokolov, A. A. Kolomenskii, G. G. Paulus, and H. A. Schuessler, Opt. Lett. **37**, 3411 (2012).
[14] J. Strohaber, J. Abul, M. Richardson, F. Zhu, A. A. Kolomenskii, and H. A. Schuessler, Opt. Express **23**, 22463 (2015).
[15] M. Hafezi, E. A. Demler, M. D. Lukin, and J. M. Taylor, Nat. Phys. **7**, 907 (2011).
[16] R. O. Umucalilar and I. Carusotto, Phys. Rev. A **84**, 043804 (2011).
[17] K. Fang, Z. Yu, and S. Fan, Phys. Rev. Lett. **108**, 153901 (2012).
[18] K. Fang, Z. Yu, and S. Fan, Nat. Photonics **6**, 782 (2012).
[19] M. C. Rechstman, J. M. Zeuner, A. Tünnermann, S. Nolte, M. Segev, and A. Szameit, Nat. Photonics **7**, 153 (2012).
[20] L. D. Tzuang, K. Fang, P. Nussenzveig, S. Fan, and M. Lipson, Nat. Photonics **8**, 701 (2014).
[21] E. Li, B. J. Eggleton, K. Fang, and S. Fan, Nat. Commun. **5**, 3225 (2014).
[22] F. Liu and J. Li, Phys. Rev. Lett. **114**, 103902 (2015).
[23] S. Raghu and F. D. M. Haldane, Phys. Rev. A **78**, 033834 (2008).
[24] F. D. M. Haldane and S. Raghu, Phys. Rev. Lett. **100**, 013904 (2008).
[25] Z. Wang, Y. D. Chong, J. D. Joannopoulos, and M. Soljačić, Phys. Rev. Lett. **100**, 013905 (2008).
[26] A. B. Khanikaev, S. H. Mousavi, W.-K. Tse, M. Kargarian, A. H. MacDonald, and G. Shvets, Nat. Mater. **12**, 233 (2013).
[27] M. C. Rechstman, J. M. Zeuner, Y. Plotnik, Y. Lumer, D. Podolsky, F. Dreisow, S. Nolte, M. Segev, and A. Szameit, Nature (London) **496**, 196 (2013).
[28] M. Hafezi, S. Mittal, J. Fan, A. Migdall, and J. M. Taylor, Nat. Photonics **7**, 1001 (2013).
[29] S. Mittal, J. Fan, S. Faez, A. Migdall, J. M. Taylor, and M. Hafezi, Phys. Rev. Lett. **113**, 087403 (2014).
[30] L. Lu, J. D. Joannopoulos, and M. Soljačić, Nat. Photonics **8**, 821 (2014).
[31] A. Celi, P. Massignan, J. Ruseckas, N. Goldman, I. B. Spielman, G. Juzeliūnas, and M. Lewenstein, Phys. Rev. Lett. **112**, 043001 (2014).
[32] X.-W. Luo, X. Zhou, C.-F. Li, J.-S. Xu, G.-C. Guo, and Z.-W. Zhou, Nat. Commun. **6**, 7704 (2014).
[33] D. Wang, H. Cai, L. Yuan, S. Zhu, and R. Liu, Optica **2**, 712 (2015).
[34] Y.-J. Lin, R. L. Compton, K. Jiménez-García, J. V. Porto, and, I. B. Spielman, Nature (London) **462**, 628 (2009).
[35] J. Dalibard, F. Gerbier, G. Juzeliūnas, and P. Öhberg, Rev. Mod. Phys. **83**, 1523 (2011).
[36] I. Bloch, J. Dalibard, and S. Nascimbène, Nat. Phys. **8**, 267 (2012).
[37] V. Peano, C. Brendel, M. Schmidt, and F. Marquardt, Phys. Rev. X **5**, 031011 (2015).
[38] F. Le Kien, K. Hakuta, and A. V. Sokolov, Phys. Rev. A **66**, 023813 (2002).
[39] From Eq. (13), Eq. (14) is valid when $q \ll k_n$. This condition is satisfied in this paper.
[40] L. Yuan, Y. Shi, and S. Fan, Opt. Lett. **41**, 741 (2016).
[41] T. Ozawa, H. M. Price, N. Goldman, O. Zilberberg, and I. Carusotto, Phys. Rev. A **93**, 043827 (2016).
[42] D. J. Thouless, M. Kohmoto, M. P. Nightingale, and M. den Nijs, Phys. Rev. Lett. **49**, 405 (1982).
[43] L. Allen and J. H. Eberly, *Optical Resonance and Two-Level Atoms* (Dover, New York, 1987).
[44] *Extreme Photonics and Applications*, edited by T. J. Hall and S. V. Gaponenko (Springer, Dordrecht, 2010).